Description of the Structure of Polystyrene with Six-Site Semiflexible Model

Qinzhi Xu, Jianguo Mi,* and Chongli Zhong

Laboratory of Computational Chemistry, Department of Chemical Engineering, Beijing University of Chemical Technology, Beijing 100029, China

Received November 26, 2008; Revised Manuscript Received January 5, 2009

ABSTRACT: In this work, a six-site semiflexible chain model for the polymer reference interaction site model (PRISM) theory was proposed and applied to describe the structure and properties of atactic polystyrene (aPS) melt. In the model, the local monomer structure is composed of six independent sites corresponding to *A* and *B* in the backbone and *C*, *D*, *E*, and *F* in the side phenyl ring group. The intramolecular correlation functions were obtained analytically with the Koyama distribution function and the generator matrix method. To improve the calculation of the intermolecular correlation functions, the potential of mean force was introduced. The calculated X-ray scattering intensity and total radial distribution function were compared with both simulation and experiment data. The results indicate that the model is an effective way to investigate the microscopic structure of styrene polymers.

1. Introduction

Styrene polymers are a class of amorphous materials with properties of both commercial and theoretical interests because of their material characteristics. Of these polymers, polystyrene is probably the most widely studied substance.[1−4] For examples, poly(cyclohexylethylene) can be obtained from the hydrogenation of polystyrene;[5] a new material of poly(cyclohexylethylene-*b*-dimethylsiloxane-*b*-cyclohexylethylene) is synthesized from poly(cyclohexylethylene).[6] Moerover, the polymeric nanocomposite system was synthesized and investigated employing polystyrene.[7,8] Understanding precisely microscopic structure of polystyrene is of great importance to the investigation of styrene polymers.

Molecular simulation has been extensively used to study the structure and properties of polystyrene. The simulation method, although quite time-consuming, usually provides exact results in modeling to compare with the experiment data. Some properties were well documented in the literatures.[1,2,5,6]

An alternative way to give a comprehensive interpretation of the polystyrene's structure and properties is the integral equation theory, or the polymer reference interaction site model (PRISM) theory.[9−11] The theory, originally based on the Flory's ideality hypothesis,[12] allows one to infer the intermolecular packing and properties of the multiple chain polymers by using the single chain structure factor. Subsequently PRISM theory was generalized to allow one to deduce both the intramolecular and intermolecular correlations in a self-consistent manner.[10,11] This can be implemented[13,14] with a semiflexible chain or rotational isomeric state chain model using a Koyama representation of the intramolecular structure factor. Later on, the theory was extended to complicated systems such as copolymers,[15] polymer nanocomposites,[16] and branched polymers. In recent years, PRISM theory was further extended to treat multisite models in a self-consistent manner[17] and applied to many realistic systems such as poly(dimethylsiloxane) melts[18] and vinyl polyolefin liquids.[19] In describing the intramolecular correlation functions of the theory, the single chain Monte Carlo simulation[17] was employed to describe the precise structure information of the systems. Furthermore, the potential of mean force was introduced to form a self-consistent computation. The calculation results are in good agreement with simulation and experiment data.

* Corresponding author. E-mail: mijg@mail.buct.edu.cn.

The above method needs simulation data as an external input and extensive iteration computation. To meet the self-consistence of theory itself and improve the computational efficiency, we feel that the accurate intramolecular correlation functions obtained theoretically is more prospective. In this work, we build on the previous work of Honnel et al.[13,14] by using a six-site semiflexible chain model to describe the detailed structure of atactic polystyrene (aPS) melt, where the bond lengths and bond angles are considered by the Koyama distribution function[20] and the generator matrix method.[21] In the six-site model, the local monomer structure is composed of six independent sites corresponding to *A* and *B* in the backbone and *C*, *D*, *E*, and *F* in the side phenyl ring group. The other two sites in the phenyl ring can be represented by *D* and *E* due to the symmetry. Within the model, the united atom force field and the parameters for aPS molecular simulation is applied directly, and the results can be tested by simulation directly. In addition, the potential of mean force is introduced to correct the original Lennard-Jones force field, and an approximate self-consistent method is constructed to improve the calculation of intermolecular correlation functions and the structure factors.

The paper is organized as follows: In the part of our theory, the six-site semiflexible chain model was described in detail, where the intramolecular correlation functions were developed theoretically and the potential of mean force was constructed; in the part of results and discussion, the intramolecular and intermolecular correlation functions, the structure factors, the X-ray scattering intensity and the total radial distribution function were presented; the conclusion was given in the final part.

2. Theory

As an extension of the reference interaction site model to polymers, PRISM theory has been extensively discussed in previous publications.[9,10,13,14] In this work, we just briefly summarize the formalism as applied to aPS with the united atom model; thus, each monomer in aPS contains eight sites. Due to the symmetry structure of the benzene, eight sites could be approximately reduced to six independent sites at a modest computational cost. As shown in Figure 1, the six sites *A*, *B*, *C*, *D*, *E*, and *F* correspond to the CH_2 and CH in the backbone, and one C atom and three CH united atoms in the side phenyl ring group, respectively.

10.1021/ma802648s CCC: $40.75
Published on Web 03/06/2009

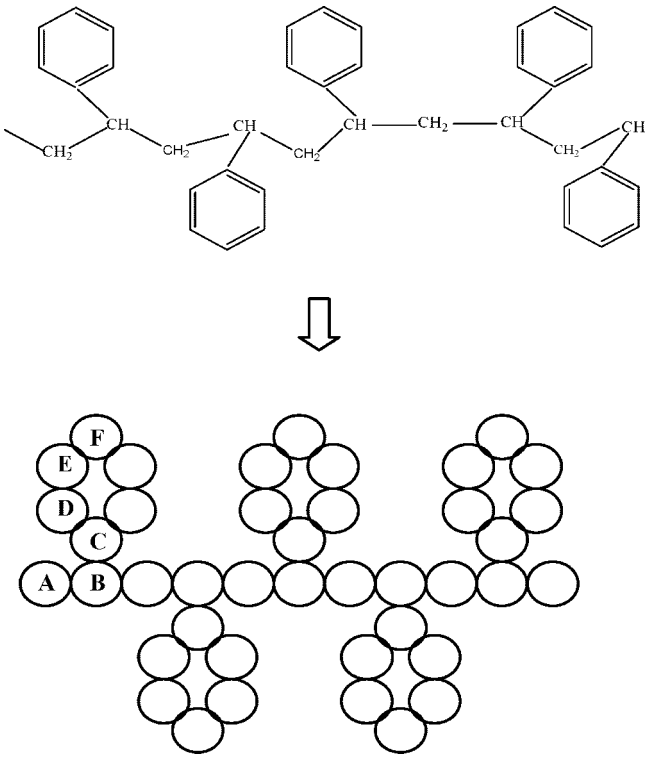

Figure 1. Graphic representation of aPS. Each monomer can be simplified to six independent sites.

For a system of N_C chains, each containing N monomers, the intermolecular packing can be characterized in terms of intermolecular correlation function $g_{\alpha\gamma}(r)$, which is defined as follows,[9]

$$\rho^2 g_{\alpha\gamma}(r) = \langle \sum_{i\neq j=1}^{N_C} \delta(\vec{r}_i^{\,\alpha})\delta(\vec{r} - \vec{r}_j^{\,\gamma})\rangle \tag{1}$$

where $\rho = N_C/V$ is the number density of molecules and $\vec{r}_i^{\,\alpha}$ is the position vector of site α on chain i. Strictly speaking, $\mathbf{g}(r)$ is a $6N \times 6N$ matrix with elements $g_{\alpha\gamma}(r)$ since each site along the chain would be distinct in the general case. Following Chandler and Andersen's definition[22,23] to multicomponent systems, a generalized matrix Ornstein−Zernike-like equation is written as

$$\mathbf{h}(r) = \int \mathrm{d}\vec{r}' \int \mathrm{d}\vec{r}''\boldsymbol{\omega}(|\vec{r} - \vec{r}'|)\mathbf{C}(|\vec{r}'-\vec{r}''|)[\boldsymbol{\omega}(r'') + \rho\mathbf{h}(r'')] \tag{2}$$

where $\mathbf{h}(r)$, $\mathbf{C}(r)$, and $\boldsymbol{\omega}(r)$ are $6N \times 6N$ matrices with elements $h_{\alpha\gamma}$,$C_{\alpha\gamma}$, and $\omega_{\alpha\gamma}$, respectively. Here, $h_{\alpha\gamma}(r)$ means the total correlation function and $h_{\alpha\gamma}(r) = g_{\alpha\gamma}(r) - 1$. $C_{\alpha\gamma}(r)$ represents the direct correlation function, and $\omega_{\alpha\gamma}(r)$ denotes the normalized intramolecular correlation function. By neglecting end effects and treating N monomers on a molecule as statistically equivalent, the total correlation functions and direct correlation functions are equivalent between any monomer from different molecules, respectively. Thereby, the compact form of Eq. (2) in Fourier space can be further expressed as

$$\hat{\mathbf{h}}(k) = \hat{\Omega}(k)\hat{\mathbf{C}}(k)[\hat{\Omega}(k) + \tilde{\rho}\hat{\mathbf{h}}(k)] \tag{3}$$

where $\tilde{\rho} = N\rho$ is the diagonal matrix of monomer density, and $\hat{h}(k)$,$\hat{C}(k)$, and $\hat{\mathbf{\Omega}}(k)$ have matrix elements $\hat{h}_{\alpha\gamma}(k)$,$\hat{C}_{\alpha\gamma}(k)$, and $\hat{\Omega}_{\alpha\gamma}(k)$. In particular, $\hat{\Omega}_{\alpha\gamma}(k)$ can be given by

$$\hat{\Omega}_{mm'}(k) = \frac{1}{N}\sum_{\alpha\in m}\sum_{\gamma\in m'}\hat{\omega}_{\alpha\gamma}(k) \tag{4}$$

where m and m' refer to the sites A, B, C, D, E, or F, and $\hat{\omega}_{\alpha\gamma}(k)$ is the Fourier transform of the intramolecular correlation function.

In order to solve eq 3 for the considered system, the standard Percus−Yevick-like closure has been used

$$C(r) = g(r)[1 - \mathrm{e}^{\beta u(r)}] \tag{5}$$

where $\beta = 1/k_B T$, $u(r)$ is the force field, and the Lennard-Jones form is employed as the original potential to describe the interactions between nonbonded sites.

$$u(r) = \varepsilon\left[\left(\frac{r_0}{r}\right)^{12} - 2\left(\frac{r_0}{r}\right)^{6}\right] \tag{6}$$

Here ε and r_0 are the site parameters.

For the worm chain, Koyama has given an approximate expression which interpolates between rigid-rod and Gaussian-coil limits while reproducing the correct second and fourth moments of the distribution. As noted by Mansfield,[24] the Koyama distribution is not limited to wormlike chains, but rather can be applied to any semiflexible model for which the second and the fourth moments $\langle r_{\alpha\gamma}{}^2\rangle$ and $\langle r_{\alpha\gamma}{}^4\rangle$ between the two points are known (provided that $\langle r_{\alpha\gamma}{}^4\rangle/\langle r_{\alpha\gamma}{}^2\rangle^2 \leq 5/3$). Thus, $\hat{\omega}_{\alpha\gamma}(k)$ in Eq. (4) can be given by[13,20]

$$\hat{\omega}_{\alpha\gamma}(k) = \frac{\sin(B_{\alpha\gamma}k)}{B_{\alpha\gamma}k}\mathrm{e}^{-A_{\alpha\gamma}{}^2k^2} \tag{7}$$

with

$$A_{\alpha\gamma}{}^2 = \langle r_{\alpha\gamma}{}^2\rangle(1 - C_{\alpha\gamma})/6 \tag{8}$$

$$B_{\alpha\gamma}{}^2 = C_{\alpha\gamma}\langle r_{\alpha\gamma}{}^2\rangle \tag{9}$$

$$C_{\alpha\gamma}{}^2 = \frac{1}{2}\left(5 - 3\frac{\langle r_{\alpha\gamma}{}^4\rangle}{\langle r_{\alpha\gamma}{}^2\rangle^2}\right) \tag{10}$$

In this work, we calculate $\langle r_{\alpha\gamma}{}^2\rangle$ and $\langle r_{\alpha\gamma}{}^4\rangle$ with the generator matrix method.[21] The mathematic derivations for this method are presented in the Supporting Information.

For the six-site model, there are only 21 independent intramolecular correlation functions needed. Because the values of $A_{\alpha\gamma}$ and $B_{\alpha\gamma}$ in eq 7 are changed with n; in this work, we use the summations to calculate the intramolecular correlation functions instead of the double integration used in freely jointed chain model. After executing the straightforward but tedious summations in eq 4, the corresponding summation equations can be obtained between the like sites as well as the unlike sites. They are given in the Supporting Information.

With the intramolecular correlation functions as input, the initial intermolecular correlation functions can be calculated with eq 3, and the corresponding structure factor $\hat{S}(k)$ can be quantified by

$$\hat{\mathbf{S}}(k) = \hat{\Omega}(k) + \tilde{\rho}\hat{\mathbf{h}}(k) = (\mathbf{I} - \tilde{\rho}\hat{\Omega}(k)\hat{\mathbf{C}}(k))^{-1}\hat{\Omega}(k) \tag{11}$$

To modify the intermolecular total correlation functions, the original Lennard-Jones potential can be corrected with the potential of mean force $W(r)$

$$u(r) = u_{\mathrm{LJ}}(r) + W(r) \tag{12}$$

where $W(r)$ can be calculated in the Fourier space

$$\beta\hat{W}_{\alpha\gamma}(k) = -\sum_{ij}\hat{C}_{\alpha i}(k)\tilde{\rho}\hat{S}_{ij}(k)\hat{C}_{j\gamma}(k) \quad (13)$$

Combining eqs 3 and 12 with eq 13, we can solve $W(r)$ by a simple Picard iteration method.[25] Under the condition of invariable intramolecular correlation functions, an approximate self-consistent theoretical method can be constructed. With the final $W(r)$, the interaction potential is corrected, and the final intermolecular correlation functions and the partial structure factors are obtained.

3. Results and Discussion

The above PRISM equations with the PY closure were solved numerically via Picard iteration using the fast Fourier transformation. For the aPS chain, the number of monomer units N was taken to be 25. The Lennard-Jones bond lengths and bond angles parameters for different sites were taken directly from the united atom AMBER force field by Weiner et al.,[26] and listed in Table 1 in the Supporting Information. It was demonstrated that, with these parameters, molecular dynamics simulations[1,4] yield nearly the same results as the experiment data.[27] Thus, the present theoretical calculation results could be compared with simulation and experiment data simultaneously.

3.1. Intramolecular Correlation Functions. The intramolecular correlation functions are crucial to PRISM theory. For like sites, the calculated results with the six-site semiflexible chain model are shown in Figure 2. While for unlike sites, some representative functions are depicted in Figure 3. As can be seen from the two figures, the general shape of the plots could be divided into three distinct regions: in the small k region, $\hat{\mathbf{\Omega}}(k)$ monotonically decreases rapidly characterizing the global dimensions of the chain; in the transitional wave vector region, $\hat{\mathbf{\Omega}}(k)$ oscillates with the decreasing magnitude; and in the outer branch, the limit of the diagonal components of $\hat{\mathbf{\Omega}}(k)$ converges to unity while the off-diagonal components converges to zero. The interesting difference between the backbone-backbone sites and the unlike sites in the phenyl ring is that the position of the first maximum peak shifts in k region differently. The possible reason of this phenomenon could be that the sites of unlike type in the phenyl ring are prone to interact with each other at the small wave vector compared to the backbone sites.

When k is small, $\hat{\omega}_{\alpha\gamma}(k)$ is proportional to k^{-2}. Therefore, $\hat{\omega}_{\alpha\gamma}(k)$ decreases rapidly. As the wave vector increases, the intermediate scaling regime begins. The intermediate scaling regime is of particular importance, as it can characterize the local chain features which can be represented partially by bond lengths and bond angles in our semiflexible model. Some qualitative characteristic of the location and shape of the transition region can be obtained by considering the behavior of a single chain. The third region of the intramolecular structure being examined is at high wavevectors, which seems to have the similar variation trend to the polyolefins.[19]

3.2. Intermolecular Correlation Functions. With the above 21 independent intramolecular correlation functions as input, the corresponding intermolecular correlation functions were calculated by the approximate self-consistent PRISM theory, in which the original force field was corrected with the potential of mean force. The intermolecular packing structures between like sites are shown in Figure 4 at $T = 500$ K with $\rho = 1.028$ g/cm^3. From the figure one can find that when the distance is larger than 14Å, all the like type correlation functions monotonically approach to unity. This region has overcome the longest length of two sites in a single macromolecule chain, and is generally called the correlation hole[27] which is a consequence of the screening of a pair of intermolecular sites on two chains.

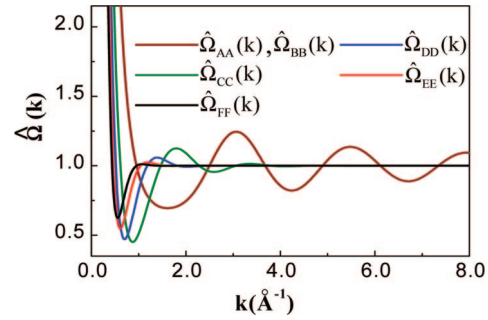

Figure 2. Intramolecular correlation functions of like sites for aPS at 500 K.

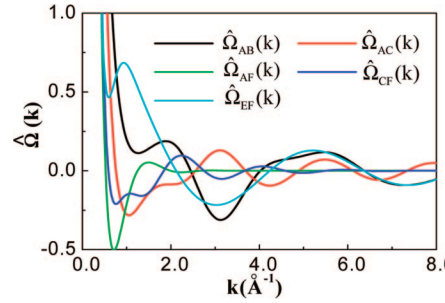

Figure 3. Intramolecular correlation functions of unlike sites for aPS at 500 K.

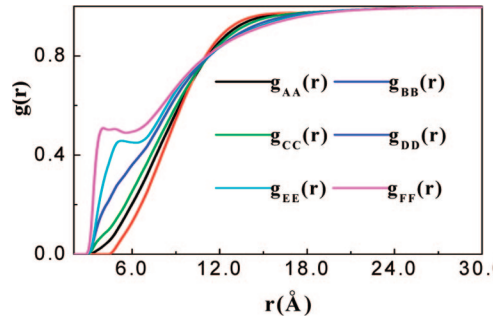

Figure 4. Intermolecular correlation functions of like sites for aPS at 500 K.

However, on short length scales, Figure 4 indicates obvious differences among the local packing correlations which depend sensitively on the local geometric structure of the monomers. The most apparent feature is an approximate plateau in the *FF* pair function at a distance just above contact; a similar but less prominent trend also appears in the *EE* correlation. The reason of these phenomena is that the phenyl ring can easily contact with each other when compared to the sites in the backbone chain, and the site *F* is located in the most exposed position. On the other hand, the *BB* pair correlation function shows unusual behavior at distances near contact, where $g_{BB}(r)$ actually becomes zero at distances greater than the distance of closest approach between two isolated *B* sites. This behavior is a consequence of the shielding of the *B* sites caused by the phenyl ring. These pair correlation functions suggest a prominent characteristic of aPS: the side group sites tend to screen out the backbone sites at short distances.

The intermolecular correlation functions of unlike sites are partially plotted in Figure 5. Again, at short distances, the relative magnitudes near contact can be explained by phenyl ring shielding arguments, although the curves are not pronounced compared to those of like ones. In the meantime, the figure shows that, in the correlation hole regime, the unlike correlation functions are essentially the same as like ones.

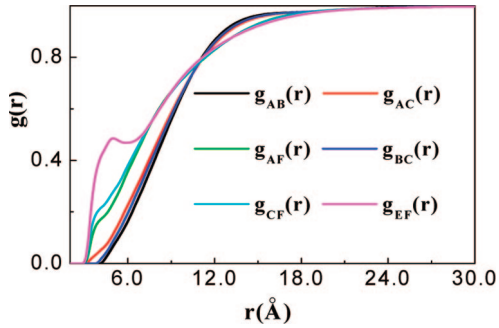

Figure 5. Intermolecular correlation functions of unlike sites for aPS at 500 K.

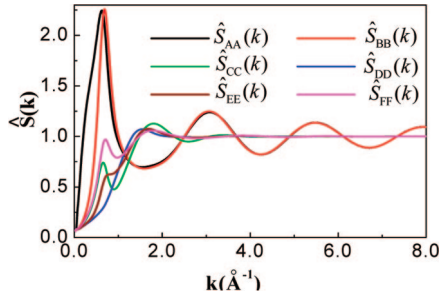

Figure 6. Structure factors of like sites as a function of wave vector k for aPS at 500 K.

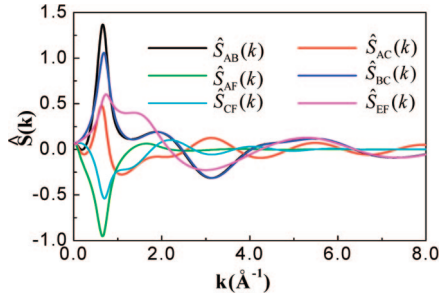

Figure 7. Structure factors of unlike sites as a function of wave vector k for aPS at 500 K.

Generally speaking, these local structural features could affect the radius of gyration and thereby influence the correlation hole.

To give insight into the structure characteristics of aPS chain, the correlation between local structure and the global dimension was further analyzed. The difference in local structure decides the second moments directly as shown in eq 8 in the Supporting Information, thereby affects the mean square radius of gyration, which describes the spatial extent of macromolecular chain. Meanwhile, the characteristic ratio C_∞, which is another important parameter for describing the flexibility of the real molecular chains, is the function of the second moments, and also correlates to the mean square radius of gyration and local structure.

3.3. Structure Factors. The corresponding partial structure factors are shown in Figure 6 for like sites, and in Figure 7 for unlike sites. It is shown that, the different and complicated behavior of the partial structure factors varies with the increasing wave vectors. The oscillatory characteristic of $\hat{S}_{\alpha\gamma}(k)$ is similar to the intramolecular correlation functions as shown in Figures 2 and 3.

3.4. X-ray Scattering Intensity. The X-ray scattering intensity $I(k)$ reflects important structure information of polymers. For PRISM theory, it can be written in terms of the elements of $\hat{S}(k)$ as follows

$$I(k) = \sum_{\alpha\gamma} b_\alpha(k) b_\gamma(k) \hat{S}_{\alpha\gamma}(k)/N_S \tag{14}$$

where N_S is the site number of each monomer, and $N_S = 8$ for aPS. $b_\alpha(k)$ is the wavevector dependent site scattering cross-section of α-type site. Following Narten's method,[28] these site scattering factors can be estimated with

$$b_\alpha(k) = \sum_{i=1}^{4} a_{\alpha i} e^{-b_{\alpha i} k^2/(16\pi^2)} + c_\alpha \tag{15}$$

where the constants $a_{\alpha i}$, $b_{\alpha i}$ and c_α are also taken from ref 28. The calculated X-ray scattering intensity of aPS is depicted in Figure 8 at $T = 413.2$ K with $\rho = 1.002$ g/cm^3, and compared with the experiment data.[29] Our result shows a lower k peak at 0.60 Å^{-1} and a higher k feature at 1.41 Å^{-1}, which has the similar location from the experiment with the so-called "polymerization peak" at 0.75 Å^{-1} and "amorphous" peak at 1.4 Å^{-1}. The intensities of the two peaks are also similar to the experiment data. In addition, another weak peak at 5.5 Å^{-1} also agrees well with the experimental value. The microscopic structure of aPS is mainly affected by the intermolecular packing of phenyl ring, which contributes to the "amorphous" peak, while the existence of the "polymerization peak" is mainly due to intermolecular correlations of backbone atoms.

To compare with molecular simulation, the reduced intensity function is employed

$$H(k) = k(I(k) - \sum x_\alpha b_\alpha{}^2(k)) \tag{16}$$

where x_α is the site fraction of species α, and $b_\alpha(k)$ is the site scattering factor determined by eq 15.

The calculated X-ray intensity curve $H(k)$ is shown in Figure 9 and compared with both the simulation[1] and experimental results.[30] It should be pointed out that, aPS contains three different configurations in the simulation[1] due to the different tacticity sequences, and the deviation between any two configurations is unobvious. In our theoretical model, tacticity and torsional angle are arbitrary; hence, we can choose any one configuration for comparison. From the figure, one can see that, although some discrepancies in the intensity of the peaks and valleys are perceivable, the overall shape of the theoretical $H(k)$ curve and the position of the main peak can match simulation and experimental curves. The deviation is probably attributed to $\hat{\mathbf{\Omega}}(k)$ calculations. In PRISM theory, monomers on a molecule are treated as statistically equivalent and the end effects are ignored. Meanwhile, in the present model, the eight sites in an aPS monomer are simplified to six sites, which inevitably miss some detailed information, and the local bending potential, the tacticity and torsional angle effects are also neglected. In addition, in our self-consistent method, $\hat{\mathbf{\Omega}}(k)$ is invariant, and this approximation neglects the effects of intermolecular interactions on it.

3.5. Total Radial Distribution Function. With the scattering intensity $I(k)$, the total radial distribution function can be expressed with

$$4\pi r^2 \delta\rho(r) = \frac{2r}{\pi} \int_0^\infty H(k)/(\sum x_\alpha b_\alpha(k))^2 M(k) \sin(kr)\, dk \tag{17}$$

where $\delta\rho(r) = \rho(r) - \rho_0$ is the deviation from the average ρ_0, and $M(k)$ is a smoothing function[31]

$$M(k) = \begin{cases} \dfrac{\sin(k\pi/k_{max})}{k\pi/k_{max}}, & k \le k_{max} \\ 0, & k > k_{max} \end{cases} \tag{18}$$

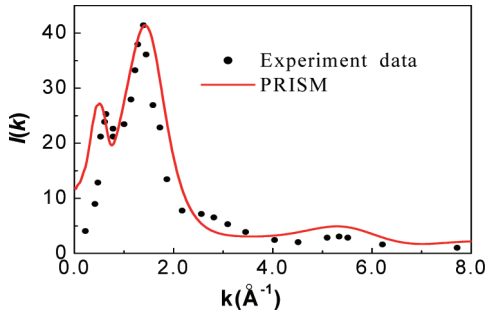

Figure 8. Comparison of the X-ray scattering intensity $I(k)$ for aPS at 413.2 K.

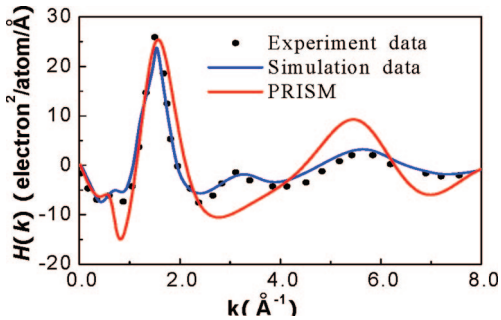

Figure 9. Comparison of the X-ray scattering intensity $H(k)$ for aPS at 500 K.

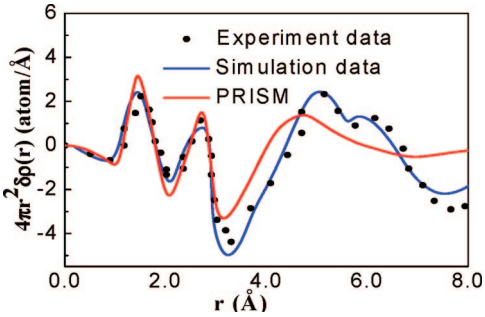

Figure 10. Comparison of total radial distribution function for aPS at 500 K.

For comparison, the calculated, simulated and experimental results are plotted in Figure 10 simultaneously. It is shown that the first and second peaks of the theoretical curve is close to both simulation[1] and experiment data.[30] The results reveal that the model can be used to display the local interaction packing and the total information of the macromolecule chain. Moreover, the reliability of the intramolecular correlation functions is validated indirectly.

4. Conclusion

In this work, a six-site semiflexible chain model was proposed to describe the structure of aPS. By introducing the united atom force field and the Koyama distribution function, the 21 intramolecular correlation functions were obtained analytically. With the intramolecular correlation functions as input to PRISM theory, the initial intermolecular correlation functions and the partial structure factors were calculated. By introducing the potential of mean force, the original force field was corrected and an approximate self-consistent method was constructed to obtain the finial intermolecular correlation functions and the structure factors. The details of chain architecture of aPS were investigated systematically. The results demonstrate that the present model can capture the complicated structure of phenyl ring without any additional input from single chain molecular simulation. This makes PRISM theory to be more convenient and self-consistent.

Considering the advantages of the new proposed model, we can expect that it can not only be used to aPS but also be extended to more complex polymers with aromatic rings contained in the side chains.

Acknowledgment. The financial support of the NSFC (20576006, 20676004, 20876007) is greatly appreciated.

Supporting Information Available: Text discussing the computational method and a table of force field parameters for the united atom model. This material is available free of charge via the Internet at http://pubs.acs.org.

References and Notes

(1) Mondello, M.; Yang, H. J.; Furuya, H.; Roe, R. J. *Macromolecules* **1994**, *27*, 3566.
(2) Ayyagari, C.; Bedrov, D.; Smith, G. D. *Macromolecules* **2000**, *33*, 6194.
(3) Spyriouni, T.; Tzoumanekas, C.; Theodorou, D.; Müller-Plathe, F.; Milano, G. *Macromolecules* **2007**, *40*, 3876.
(4) Sun, Q.; Faller, R *J. Phys. Chem. B.* **2005**, *109*, 15714.
(5) Gehlsen, M. D.; Bates, F. S. *Macromolecules* **2003**, *26*, 4122.
(6) Maheshwari, S.; Tsapatsis, M; Bates, F. S. *Macromolecules* **2007**, *40*, 6638.
(7) Harth, E.; Horn, B. V.; Lee, V. Y.; Germack, D. S.; Gonzales, C. P.; Miller, R. D.; Hawker, C. J. *J. Am. Chem. Soc.* **2002**, *124*, 8653.
(8) Mackay, M. E.; Dao, T. T.; Tuteja, A.; Ho, D. L.; Horn, B. V.; Kim, H. C.; Hawker, C. J. *Nat. Mater.* **2003**, *2*, 762.
(9) Schweizer, K. S.; Curro, J. G. *Phys. Rev. Lett.* **1987**, *58*, 246.
(10) Schweizer, K. S.; Curro, J. G. *Adv. Chem. Phys.* **1997**, *98*, 1.
(11) Heine, D. R.; Grest, G. S.; Curro, J. G. *Adv. Polym. Sci.* **2005**, *173*, 209.
(12) Flory, P. J. *J. Chem. Phys.* **1949**, *17*, 203.
(13) Honnell, K. G.; Curro, J. G.; Schweizer, K. S. *Macromolecules* **1990**, *23*, 3496.
(14) Schweizer, K. S.; Honnell, K. G.; Curro, J. G. *J. Chem. Phys.* **1992**, *96*, 3211.
(15) Sung, B. J.; Yethiraj, A. *Macromolecules* **2000**, *38*, 2000.
(16) Hooper, J. B; Schweizer, K. S. *Macromolecules* **2006**, *39*, 5133.
(17) Ptz, M.; Curro, J. G.; Grest, G. S. *J. Chem. Phys.* **2001**, *114*, 2847.
(18) Habenschuss, A.; Tsige, M.; Curro, J. G.; Grest, G. S.; Nath, S. K. *Macromolecules* **2007**, *40*, 7036.
(19) Li, H.; Curro, J. G.; Wu, D. T.; Habenschuss, A. *Macromolecules* **2008**, *41*, 2694.
(20) Koyama, R. *J. Phys. Soc. Jpn.* **1973**, *34*, 1029.
(21) Flory, P. J. *Macromolecules* **1974**, *7*, 381.
(22) Chandler, D.; Andersen, H. C. *J. Chem. Phys.* **1972**, *57*, 1930.
(23) Chandler, D. In *Studies in Statistical Mechanics VIII*; Montroll, E. W., Lebowitz, J. L., Eds.; North-Holland: Amsterdam, 1982.
(24) Mansfield, M. L. *Macromolecules* **1986**, *19*, 854.
(25) Hansen JP, J. P.; McDonald I. R. *Theory of simple liquids[M]*, 2nd ed.; Academic: London, 1986.
(26) Weiner, S. J.; Kollman, P. A.; Case, D. A.; Singh, U. C.; Chio, C.; Alagona, G.; Profeta, S. J.; Weiner, P. *J. Am. Chem. Soc.* **1984**, *106*, 765.
(27) de Gennes, P. G. *Scaling Concepts in Polymer Physics*; Cornell University Press: Ithaca, NY, 1979.
(28) Narten, A. *J. Chem. Phys.* **1979**, *70*, 299.
(29) Song, H. H.; Roe, R. J. *Macromolecules* **1987**, *20*, 2723.
(30) Mitchell, G. R.; Windle, A. H. *Polymer* **1984**, *25*, 906.
(31) Schubach, H. R; Nagy, E; Heise, B. *Colloid Polym. Sci.* **1982**, *259*, 789.

MA802648S